Medicinal Chemistry

DOI: 10.1002/anie.201311162

Deorphaning Pyrrolopyrazines as Potent Multi-Target Antimalarial Agents**

*Daniel Reker, Michael Seet, Max Pillong, Christian P. Koch, Petra Schneider, Matthias C. Witschel, Matthias Rottmann, Céline Freymond, Reto Brun, Bernd Schweizer, Boris Illarionov, Adelbert Bacher, Markus Fischer, François Diederich, and Gisbert Schneider**

Abstract: *The discovery of pyrrolopyrazines as potent antimalarial agents is presented, with the most effective compounds exhibiting EC_{50} values in the low nanomolar range against asexual blood stages of Plasmodium falciparum in human red blood cells, and Plasmodium berghei liver schizonts, with negligible HepG2 cytotoxicity. Their potential mode of action is uncovered by predicting macromolecular targets through avant-garde computer modeling. The consensus prediction method suggested a functional resemblance between ligand binding sites in non-homologous target proteins, linking the observed parasite elimination to IspD, an enzyme from the non-mevalonate pathway of isoprenoid biosynthesis, and multi-kinase inhibition. Further computational analysis suggested essential P. falciparum kinases as likely targets of our lead compound. The results obtained validate our methodology for ligand- and structure-based target prediction, expand the bioinformatics toolbox for proteome mining, and provide unique access to deciphering polypharmacological effects of bioactive chemical agents.*

Malaria poses a severe health threat, and the rising emergence of multi drug-resistant pathogens underlines the urgent necessity of drug development with innovative modes of action.[1–3] Herein, we disclose the identification of unique antimalarial agents with nanomolar growth inhibition effect on *P. falciparum*. We demonstrate how computational methods can be efficiently used to reveal their potential mechanism of action. Pursuing a rigorous sequence- and structure-based bioinformatics procedure, the approach starts from identifying human targets and then makes the transition to potential *P. falciparum* targets by orthologous identification and experimental validation.[4–7]

Initially, we discovered pyrroloquinoxaline **1** (Figure 1) in a high-throughput screening (HTS) campaign performed at BASF, which aimed at finding low-molecular-weight compounds that inhibit the herbicidal target 4-diphosphocytidyl-2*C*-methyl-D-erythritol synthase (IspD) from the plant *Ara-*

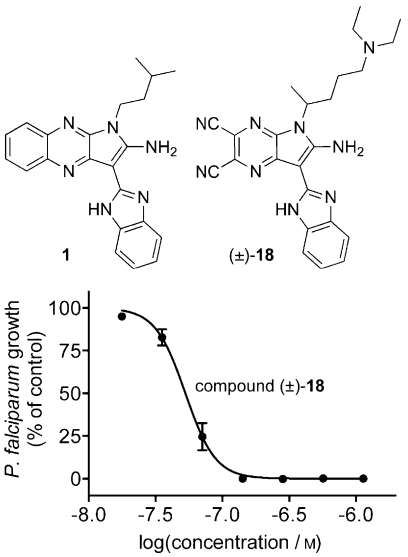

Figure 1. Structures of reference compound **1** (IC_{50} *A. thaliana* IspD = 1.6 μM) and lead compound (±)-**18**, and concentration-dependent growth inhibition of drug-sensitive *P. falciparum* NF54 parasites by compound (±)-**18**. Untreated parasite growth served as control (= 100%). $n = 4$ (two independent experiments with two technical replicates); mean ± SEM.

[*] D. Reker,[+] Dr. M. Seet,[+] M. Pillong, Dr. C. P. Koch, Dr. P. Schneider, Dr. B. Schweizer, Prof.Dr. F. Diederich, Prof. Dr. G. Schneider
Departement Chemie und Angewandte Biowissenschaften
ETH Zürich, Vladimir-Prelog-Weg 3-4, 8093 Zürich (Switzerland)
E-mail: gisbert.schneider@pharma.ethz.ch

Dr. M. C. Witschel
BASF SE, Boschstrasse 14, 67056 Ludwigshafen (Germany)

Dr. M. Rottmann, C. Freymond, Prof. Dr. R. Brun
Schweizerisches Tropen- und Public-Health Institut
Socinstrasse 57, 4051 Basel (Switzerland)
and
Universität Basel, Petersplatz 1, 4003 Basel (Switzerland)

Dr. B. Illarionov, Prof. Dr. A. Bacher, Prof. Dr. M. Fischer
Universität Hamburg, Hamburg School of Food Science
Institut für Lebensmittelchemie
Grindelallee 117, 20146 Hamburg (Germany)

Dr. P. Schneider, Prof. Dr. G. Schneider
inSili.com GmbH
Segantinisteig 3, 8049 Zürich (Switzerland)

[+] These authors contributed equally to this work.

[**] We thank Dr. Case McNamara for support and discussion, and Dr. Michael D. Wörle for help with the X-ray crystal structures. This work was supported by a grant from the ETH research council and F. Hoffmann-La Roche, Ltd, by BASF SE, Ludwigshafen, and the OPO Foundation Zürich.

Supporting information for this article (including experimental procedures, chemical synthesis, cytotoxicity data, spectral data, assay conditions, X-ray data, and detailed computational methods and results) is available on the WWW under http://dx.doi.org/10.1002/anie.201311162.

bidopsis thaliana.[8,9] A large set of derivatives was synthesized and tested, but none of the follow-up compounds exhibited lower than micromolar IC_{50} values against *A. thaliana* IspD. We decided to transfer the observed moderate activity of the HTS hits from the plant IspD enzyme to a potential antimalarial application, because IspD is essential for the survival of *Plasmodium spp*.[10] Plants and *Apicomplexa* such as malaria parasites possess the ability to produce isoprenoids via the non-mevalonate pathway as an alternative to the classical hydroxymethylglutaryl-CoA reductase route. In fact, IspD as an integral enzyme of the non-mevalonate route is an attractive drug target for antimalaria research because there is no human IspD homologue.

As no direct inhibition assay with purified *plasmodial* IspD was available, we tested compound **1** in a phenotypic assay against asexual blood stages of the drug-sensitive *P. falciparum* NF54 strain. We observed almost complete inhibition of parasite growth (> 99% inhibition) at a compound concentration of 0.5 $\mu g\,mL^{-1}$, which corresponds to an EC_{50} value of approximately 200 nM. Further chemical optimization of the initial hit revealed improved growth inhibition when the quinoxaline core was replaced by a dicyanopyrazine. In total, we synthesized and tested a set of 32 derivatives. The results for compounds **2**–(±)-**33** show a remarkable antimalarial potential of this substance class (Table 1). Synthesis of all derivatives followed a two-step route (Scheme 1). Commercially available pyrazine derivative **34** was substituted by acetonitrile derivatives **35**–**37** to give **38**–**40** with subsequent formation of the pyrrole ring upon treatment with a primary amine under basic conditions.[11,12]

In the cell-based assay, almost all pyrrolopyrazines tested in our study turned out to be strongly active against *P. falciparum*, with EC_{50} values in the nanomolar range. To assess the cytotoxicity of the compounds, they were tested on rat skeletal myoblasts (L6 cells) as a mammalian model system. The selectivity index (SI) was expressed as the ratio of EC_{50} on L6 cells versus EC_{50} against *Plasmodium*. As a general trend, we observed that the aromatic side chains ensure low cytotoxicity with acceptable activity against *Plasmodium*, while derivatives with basic side chains seem to be the most active ones. Pyrrolopyrazines (±)-**18** and (±)-**20** in particular exhibited strong antiplasmodial activity, with EC_{50} values in the double-digit nanomolar range (Table 1). The selected lead compound (±)-**18** (*P. falciparum* NF54 $EC_{50} = 53$ nM; $\Delta pEC_{50} = 0.02$ log units; Figure 1) features a side chain resembling the one from chloroquine, with adequate selectivity (SI = 40), and remarkable lipophilic ligand efficiency[13,14] (LLE = 4.0). We also tested this lead against the chloroquine-resistant *P. falciparum* K1 strain, yielding an EC_{50} value of 40 nM ($\Delta pEC_{50} = 0.75$ log units). Of note, this substance also exhibited strong inhib-

Table 1: Structure, antiplasmodial activity (NF54 strains) and cytotoxicity (L6 cells) of pyrrolopyrazines **2**–(±)-**33**.[a]

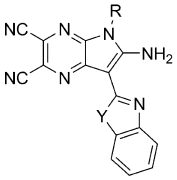

	R	Y	EC_{50} [μM] (NF54)	EC_{50} [μM] (L6)	SI	LLE
2		NH	0.25	85	348	3.5
3	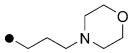	NH	0.28	3	11	5.3
4	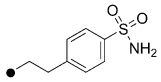	NH	> 100	> 100	n.a.	n.a.
5	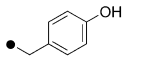	NH	0.29	4	13	3.6
6	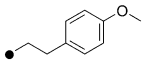	NH	0.16	174	1093	3.6
7	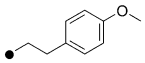	NMe	4.80	188	39	1.7
8	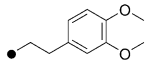	NH	0.25	148	591	3.7
9	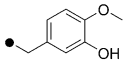	NH	1.27	187	148	3.1
10	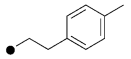	NH	0.26	141	625	3.1
11	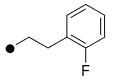	NH	0.41	80	198	3.0
12	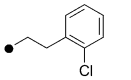	NH	0.28	143	519	2.7
13	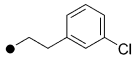	NH	0.19	52	273	2.9
14	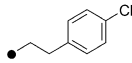	NH	0.22	40	182	2.8
15		NH	0.14	6	42	5.6
16	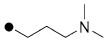	NH	0.10	1	14	5.3
17	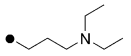	NH	0.09	1	11	4.7
(±)-**18**	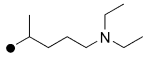	NH	0.05	2	40	4.0
(±)-**19**	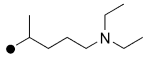	NMe	0.34	12	37	2.8
(±)-**20**	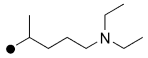	S	0.04	9	210	3.2
21	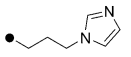	NH	0.30	> 100	> 820	5.0
22	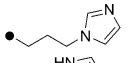	S	0.59	18	30	3.8
23	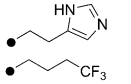	NH	0.12	4	34	6.0
24	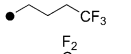	NH	0.74	81	109	3.1
25	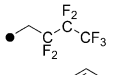	NH	0.36	42	116	3.3
26	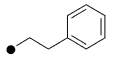	NH	0.28	55	194	3.3

Table 1: (Continued)

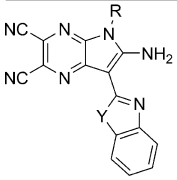

	R	Y	EC_{50} [μM] (NF54)	EC_{50} [μM] (L6)	SI	LLE
27	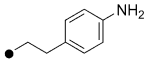	NH	0.53	158	301	3.7
28	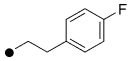	NH	0.32	129	401	3.1
29	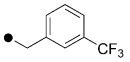	NH	0.18	13	72	2.6
30	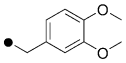	NH	1.98	100	51	2.9
31	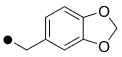	NH	0.32	53	158	3.6
32	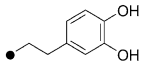	NH	5.23	22	4	2.6
(±)-**33**	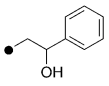	NH	0.44	16	36	3.8

[a] SI: selectivity index, LLE: lipophilic ligand efficiency.

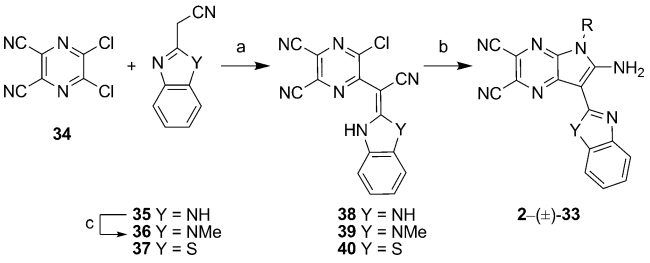

Scheme 1. General synthetic strategy. a) DMF, 40 °C, 3–4 h; b) RNH_2, NEt_3, DMF, 50–70 °C, 2–23 h; c) Me_2SO_4, K_2CO_3, DMF, 40 °C, 10 h.

itory activity against the liver schizont stage of *P. berghei* ($EC_{50} = 0.3 \pm 0.1$ μM) and did not show cytotoxicity against HepG2 cell cultures over a period of 48 h.

The discrepancy between the expected activity of the compounds in the low micromolar range, as we inferred from the *A. thaliana* IspD results, and the low nanomolar EC_{50} values against *Plasmodium* suggest a different or additional mechanism of action. Consequently, we computationally predicted potential macromolecular targets of lead structure (±)-**18**. We used a self-organizing map (SOM)[15] that was trained to cluster 11827 drugs and bioactive lead compounds that are known to bind to a total of 673 macromolecular targets comprising 212 target and activity families.[16–18] The SOM groups molecules with similar pharmacophoric features into clusters of functionally related compounds.[19,20] Compound (±)-**18** was projected onto this map, and from the known targets of the co-clustered drug molecules we statistically inferred its potential targets. Following this concept, we previously identified new targets for old drugs,[21,22] and successfully "deorphaned" combinatorial compound libraries.[23] Background inter-target compound similarities were used to rationalize similarities between (±)-**18** and the co-clustered drug molecules by ranking predictions according to their false-positive error probability.[20] Retrospective evaluation demonstrated that such a scoring scheme is remarkably well-suited for making true-positive predictions, yielding an average receiver-operator characteristic (ROC) area-under-curve (AUC)[24] value of 0.78 ± 0.14 in 10-fold cross validation on the level of 212 target families, with AUC values of up to 1.0 for individual targets (Supporting Information, Table S13). Calculating rank scores for background data allowed us to compute conservative *p*-values.[25] Table 2 presents the suggested target list for compound (±)-**18** with $p < 0.1$. The predictions clearly implied kinases as potential targets. This result is in line with a study published by Volovenko and coworkers,[26] who hypothesized, on the basis of an observed general antiproliferative potential of pyrrolopyrazines, a binding mode of these compounds to the hinge region of several kinases.

In an attempt to biochemically probe for the computationally predicted kinase inhibition, we subjected compound (±)-**18** and selected analogues

Table 2: Top-ranking (*p* value < 10%) predicted targets and target classes for compound (±)-**18**.

Rank	Predicted target	*p* value [%]
1	thrombin receptor	7.2
2	serine-threonine kinase	8.7
3	adenosine kinase	9.1
4	tyrosine kinase	9.6
5	growth-hormone-releasing peptide receptor	9.7
6	DNA topoisomerase	9.9

6, **8**, and **16** to activity testing in a human kinase panel (Cerep ExpresS diversity kinase profile; Table 3). Compound (±)-**18** inhibited 21 out of 48 tested kinases with > 50% effect at a testing concentration of 10 μM. The basic derivative **16** showed a slightly weaker overall inhibitory effect (17/48), and pyrrolopyrazines **6** and **8**, featuring an aromatic side chain and weaker antiplasmodial activity, exhibited no observable kinase inhibition. For the four kinases that were inhibited with ≥ 99% efficiency by compound (±)-**18**, IC_{50} values were determined. Low single-digit micromolar values corroborate the target prediction, specifically for insulin receptor protein-tyrosine kinase (IRK): 2.5 μM, serine-threonine-protein kinase RAF-1: 2.3 μM, tyrosine protein kinases Src: 2.3 μM, and tropomyosin receptor kinase TrkA: 1.0 μM (*SEM* < 1 log unit for all IC_{50} values; Figure 2A). These results designate members of the pyrrolopyrazine class as potent kinase inhibitors and uphold our working hypothesis that the observed high antiplasmodial activity of compound (±)-**18** might be caused at least in part by multi-target effects.

The measured human kinase inhibition offers only an indirect explanation for the observed antiplasmodial activity, as plasmodial homologues of the inhibited kinases are yet

Table 3: Inhibition of human kinases by pyrrolopyrazines **6**, **8**, **16**, and (±)-**18** at a concentration of 10 μM (n=2).[a]

Kinase	Compound number			
	6	**8**	**16**	(±)-**18**
Abl	–	–	78	–
Akt1/PKBα	–	interf.	92	74
CDK2	–	–	76	–
CHK1	–	–	71	–
CHK2	–	–	–	91
CK1α	–	–	97	73
c-Met	–	interf.	82	88
EGFR	–	–	–	88
EphA2	–	–	91	–
FGFR2	–	–	77	95
FGFR3	–	–	–	70
IKKα	–	–	80	94
IRK (InsR)	–	–	81	99
JAK3	–	–	77	interf.
Lck kinase	–	–	–	78
MKK6	–	–	-	88
MNK2	–	interf.	–	92
MST4	–	–	80	92
Pim2	–	interf.	78	96
PKA	–	–	–	83
PKCβ2	–	–	59	95
RAF-1	–	–	–	100
SGK1	–	–	84	91
SIK	–	–	–	91
Src	–	–	95	99
TrkA	–	–	98	99

[a] Targets are listed for which more than 50% inhibition was observed (interf.: interference with the assay read-out).

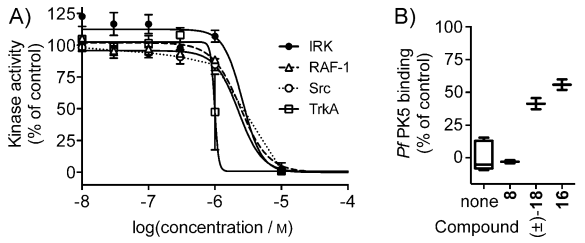

Figure 2. A) Concentration-dependent inhibition of human kinase activity by compound (±)-**18** (n=2); positive control: staurosporin. B) qPCR signal of DNA-labeled *P. falciparum* protein kinase 5 (*Pf*PK5) after adding 30 μM test compound (n=2 technical replicates) to compete with immobilized reference ligand.

unknown. At the same time, one might consider antikinase activity a possible explanation for the observed cytotoxicity (EC_{50}=2 μM for (±)-**18**; Table 1), as rat myoblasts contain homologues of the strongly inhibited kinases with more than 90% sequence identity, and we observed lower cytotoxicity for selected derivatives that do not show measurable kinase inhibition. In an effort to elucidate potential *P. falciparum* target kinases of inhibitor (±)-**18**, we firstly performed a rigorous sequence-based computational search (Supporting Information, Table S14). To this end, we locally aligned the complete amino acid sequences of the four most strongly inhibited human kinases (IRK, RAF-1, Src, TrkA) with all plasmodial proteins annotated in PlasmoDB (v9.3) for *P. falciparum* strains 37D and IT using the basic local alignment search tool (BLAST).[27] We focused on local sequence motifs in plasmodial proteins that were hit by all of the four query kinase sequences to probe for a common binding site. This consensus approach retrieved a total of 36 plasmodial subsequences from 30 proteins with statistically significant maximal expect (E)-values $<10^{-5}$ for all four searches (E-value: the number of hits that can be expected to be seen by chance). Remarkably, half of the hits belong to kinase families that were previously reported as essential for the parasite, confirmed in knockout studies, and suggested as targets for innovative antiplasmodial therapy, for example, NimA ("never in mitosis" A)-related, calcium-dependent and cyclin-dependent kinases.[28]

As a consequent extension of the initial sequence-based analysis, we performed a structure-based search for matching protein surface cavities. As a consequence of the observed multikinase inhibition, we focused on the nucleotide-binding pockets from the four human kinases that were fully inhibited by compound (±)-**18** in the panel assay (PDB IDs:[29] 3omv for RAF-1, 4aoj for TrkA, 4ibm for IRK, 2src for Src), and all seven *P. falciparum* kinases, for which X-ray structures were available from the PDB (PDB IDs: 1ltk, 1v0p, 1z6g, 2w41, 2wwf, 2yog, 3q5i). The software PoLiMorph[30] compares the shape and properties of protein surface cavities by converting the pocket volumes to branched graphs (so-called pocket graphs) that are labeled by the local hydrogen-bonding, hydrophobic, and electrostatic potentials, and their buriedness and surface accessibility. These graphs are compared by applying a deterministic matching algorithm to obtain pairwise similarity scores.[31] Significant pocket similarity scores were observed for *Pf*PK5[32] matching with human RAF-1, TrkA, and IRK. Subsequently, we compared *Pf*PK5 to its human homologue CDK2 in both the cyclin-activated (PDB ID: 1fin) and the inactive (PDB ID: 4fko) state (Supporting Information, Figure S3). Both comparisons yielded significant similarity scores, and both CDK2 pockets exhibited comparable screening results against the previously selected human kinase panel (Supporting Information, Table S15).

Because of this putative pharmacophoric pocket similarity, the retrieval of *Pf*PK5 in the sequence-based search, and the observed moderate inhibitory activity of compounds **16** and (±)-**18** (76% and 26% inhibition at 10 μM, n=2) against the human homologue CDK2, we selected compound (±)-**18** and its analogues **8** and **16** for a competitive *Pf*PK5 binding assay. Both **16** and (±)-**18** exhibited moderate but significant binding to *Pf*PK5 at a concentration of 30 μM, while the negative control **8** showed no effect (Figure 2B). Of note, all three compounds did not bind to *Pf*CDPK1 in a counterscreen (data not shown). This result validates the computational target identification and suggests binding of our lead structure to the active site of *Pf*PK5. Evidently, these preliminary binding data do not warrant the relevance of *Pf*PK5 inhibition by compound (±)-**18** in vivo. Quantification of histone H1 phosphorylation in parasites together with in vitro evolution and comparative genomic analysis might help to obtain further evidence.[33]

The pyrrolopyrazine, which was initially discovered in a high-throughput screen on the herbicidal target IspD, proved to show remarkable antiplasmodial activity. Optimi-

zation of the cell-based activity revealed low-nanomolar lead compound (±)-**18**. Advanced ligand-, protein sequence-, and pocket-based computational studies were applied in concert, and the results suggested essential plasmodial kinases as potential targets of this compound class. In fact, multiple-target inhibition has been proposed as a resistance-robust antiplasmodial strategy,[34] and the here identified kinase *Pf*PK5 has previously been suggested as a candidate target of efficient multi-target drugs.[7] Our study demonstrates that chemistry-based target inference ideally complements and inspires biochemical proteome mining and chemical genetics. By pointing out subtle functional relationships between ligand classes, the prediction method supplements other computational tools and provides a fresh view on ligand-target association.

Experimental Section

Ligand-based target prediction: Drug molecules (collection of bioactive reference compounds, COBRA v. 11.10)[16] and lead compound (±)-**18** were pre-processed using the "wash" function within the molecular operating environment (MOE 2011.10),[35] with options "disconnect salts", "remove ion pairs", "deprotonate strong acids", "remove minor components", "protonate strong bases", and "add hydrogen". Molecules were subsequently represented by topological pharmacophores ("CATS2" descriptor) and clustered by SOM training using our own software tools, as previously described.[17,20] Computational analysis investigated similarities of drugs to (±)-**18** in terms of their pharmacophoric features, and transformed them into false-positive probabilities using background statistics of distances between molecules of the COBRA database annotated to bind different targets. Calculation of average false-positive probabilities led to a rank ordering according to prediction confidence.[22]

Kinase assays: In vitro data for human kinases were obtained at Cerep (86600 Celle l'Evescault, France; http://www.cerep.fr) on a fee-for-service basis. Binding affinities of selected compounds for *Pf*PK5 were obtained at DiscoverX (San Diego, CA USA; http://www.discoverx.com) in their KINOMEscan assay on a fee-for-service basis.

Received: December 23, 2013
Revised: March 6, 2014
Published online: June 4, 2014

Keywords: computer-assisted drug design · isoprenoid synthase · kinases · medicinal chemistry · target prediction

[1] WHO World Malaria Report **2012**, http://www.who.int/malaria/publications/world_malaria_report_2012/en/.
[2] a) C. J. Murray, L. C. Rosenfeld, S. S. Lim, K. G. Andrews, K. J. Foreman, D. Haring, N. Fullman, M. Naghavi, R. Lozano, A. D. Lopez, *Lancet* **2012**, *379*, 413 – 431; b) B. Greenwood, T. Mutabingwa, *Nature* **2002**, *415*, 670 – 672; c) J. Sachs, P. Malaney, *Nature* **2002**, *415*, 680 – 685.
[3] M. Bassetti, M. Merelli, C. Temperoni, A. Astilean, *Ann. Clin. Microbiol. Antimicrob.* **2013**, *12*, 22.
[4] D. Plouffe, A. Brinker, C. McNamara, K. Henson, N. Kato, K. Kuhen, A. Nagle, F. Adrián, J. T. Matzen, P. Anderson, T. Nam, N. S. Gray, A. Chatterjee, J. Janes, S. F. Yan, R. Trager, J. S. Caldwell, P. G. Schultz, Y. Zhou, E. A. Winzeler, *Proc. Natl. Acad. Sci. USA* **2008**, *105*, 9059 – 9064.
[5] K. Jensen, D. Plichta, G. Panagiotou, I. Kouskoumvekaki, *Mol. BioSyst.* **2012**, *8*, 1678 – 1685.
[6] F.-J. Gamo, L. M. Sanz, J. Vidal, C. Cozar, E. Alvarez, J.-L. Lavandera, D. E. Vanderwall, D. V. S. Green, V. Kumar, S. Hasan, J. R. Brown, C. E. Peishoff, L. R. Cardon, J. F. Garcia-Bustos, *Nature* **2010**, *465*, 305 – 310.
[7] A. Spitzmüller, J. Mestres, *PLoS Comput. Biol.* **2013**, *9*, e1003257.
[8] V. Illarionova, J. Kaiser, E. Ostrozhenkova, A. Bacher, M. Fischer, W. Eisenreich, F. Rohdich, *J. Org. Chem.* **2006**, *71*, 8824 – 8834.
[9] A. Bacher, M. H. Zenk, W. Eisenreich, F. Fellermeier, M. Fischer, S. Hecht, S. Herz, K. Kis, H. Lüttgen, F. Rohdich, S. Sagner, C. A. Schuhr, J. Wungsintaweekul, WO 2001011055, **2001**.
[10] a) M. J. Gardner, N. Hall, E. Fung, O. White, M. Berriman, R. W. Hyman, J. M. Carlton, A. Pain, K. E. Nelson, S. Bowman, I. T. Paulsen, K. James, J. A. Eisen, K. Rutherford, S. L. Salzberg, A. Craig, S. Kyes, M.-S. Chan, V. Nene, S. J. Shallom, B. Suh, J. Peterson, S. Angiuoli, M. Pertea, J. Allen, J. Selengut, D. Haft, M. W. Mather, A. B. Vaidya, D. M. A. Martin, A. H. Fairlamb, M. J. Fraunholz, D. S. Roos, S. A. Ralph, G. I. McFadden, L. M. Cummings, G. M. Subramanian, C. Mungall, J. C. Venter, D. J. Carucci, S. L. Hoffman, C. Newbold, R. W. Davis, C. M. Fraser, B. Barrell, *Nature* **2002**, *419*, 498 – 511; b) W. Eisenreich, A. Bacher, D. Arigoni, F. Rohdich, *Cell. Mol. Life Sci.* **2004**, *61*, 1401 – 1426; c) M. Rohmer, *Nat. Prod. Rep.* **1999**, *16*, 565 – 574; d) M. Witschel, M. Rottmann, M. Kaiser, R. Brun, *PLoS Neglected Trop. Dis.* **2012**, *6*, e1805.
[11] Y. M. Volovenko, *Chem. Heterocycl. Compd.* **1998**, *34*, 171 – 173.
[12] Y. M. Volovenko, G. G. Dubinina, *Chem. Heterocycl. Compd.* **1999**, *9*, 1089 – 1095.
[13] G. M. Keserü, G. M. Makara, *Nat. Rev. Drug Discovery* **2009**, *8*, 203 – 212.
[14] M. M. Hann, G. M. Keserü, *Nat. Rev. Drug Discovery* **2012**, *11*, 355 – 365.
[15] T. Kohonen, *Biol. Cybern.* **1982**, *43*, 59 – 69.
[16] P. Schneider, G. Schneider, *QSAR Comb. Sci.* **2003**, *22*, 713 – 718.
[17] P. Schneider, Y. Tanrikulu, G. Schneider, *Curr. Med. Chem.* **2009**, *16*, 258 – 266.
[18] G. Schneider, Y. Tanrikulu, P. Schneider, *Future Med. Chem.* **2009**, *1*, 213 – 218.
[19] G. Schneider, W. Neidhart, T. Giller, G. Schmid, *Angew. Chem.* **1999**, *111*, 3068 – 3070; *Angew. Chem. Int. Ed.* **1999**, *38*, 2894 – 2896.
[20] M. Reutlinger, C. P. Koch, D. Reker, N. Todoroff, P. Schneider, T. Rodrigues, G. Schneider, *Mol. Inf.* **2013**, *32*, 133 – 138.
[21] a) R. Steri, P. Schneider, A. Klenner, M. Rupp, M. Schubert-Zsilavecz, G. Schneider, *Mol. Inf.* **2013**, *29*, 287 – 292; b) J. Lötsch, G. Schneider, D. Reker, M. J. Parnham, P. Schneider, G. Geisslinger, A. Doehring, *Trends Mol. Med.* **2013**, *19*, 742 – 753.
[22] D. Reker, T. Rodrigues, P. Schneider, G. Schneider, *Proc. Natl. Acad. Sci. USA* **2014**, *111*, 4067 – 4072.
[23] S. Renner, M. Hechenberger, T. Noeske, A. Böcker, C. Jatzke, M. Schmuker, C. G. Parsons, T. Weil, G. Schneider, *Angew. Chem.* **2007**, *119*, 5432 – 5435; *Angew. Chem. Int. Ed.* **2007**, *46*, 5336 – 5339.
[24] T. A. Alonzo, M. S. Pepe, *Methods Mol. Biol.* **2007**, *404*, 89 – 116.
[25] P. Baldi, R. Nasr, *J. Chem. Inf. Model.* **2010**, *50*, 1205 – 1222.
[26] G. G. Dubinina, M. O. Platonov, S. M. Golovach, P. O. Borysko, A. O. Tolmachov, Y. M. Volovenko, *Eur. J. Med. Chem.* **2006**, *41*, 727 – 737.
[27] S. F. Altschul, W. Gish, W. Miller, E. W. Myers, D. J. Lipman, *J. Mol. Biol.* **1990**, *215*, 403 – 410.
[28] L. Solyakov, J. Halbert, M. M. Alam, J.-P. Semblat, D. Dorin-Semblat, L. Reininger, A. R. Bottrill, S. Mistry, A. Abdi, C. Fennell, Z. Holland, C. Demarta, Y. Bouza, A. Sicard, M.-P. Nivez, S. Eschenlauer, T. Lama, D. C. Thomas, P. Sharma, S.

Agarwal, S. Kern, G. Pradel, M. Graciotti, A. B. Tobin, C. Doerig, *Nat. Commun.* **2011**, *2*, 565.
[29] H. M. Berman, J. Westbrook, Z. Feng, G. Gilliland, T. N. Bhat, H. Weissig, I. N. Shindyalov, P. E. Bourne, *Nucleic Acids Res.* **2000**, *28*, 235 – 242.
[30] F. Reisen, M. Weisel, J. M. Kriegl, G. Schneider, *J. Proteome Res.* **2010**, *9*, 6498 – 6510.
[31] M. Weisel, J. M. Kriegl, G. Schneider, *ChemBioChem* **2010**, *11*, 556 – 563.
[32] L. S. Brinen, T. J. Stout, *Structure* **2003**, *11*, 1309 – 1310.
[33] a) K. Le Roch, C. Sestier, D. Dorin, N. Waters, B. Kappes, D. Chakrabarti, L. Meijer, C. Doerig, *J. Biol. Chem.* **2000**, *275*, 8952 – 8958; b) C. W. McNamara, M. C. Lee, C. S. Lim, S. H. Lim, J. Roland, A. Nagle, O. Simon, B. K. Yeung, A. K. Chatterjee, S. L. McCormack, M. J. Manary, A. M. Zeeman, K. J. Dechering, T. R. Kumar, P. P. Henrich, K. Gagaring, M. Ibanez, N. Kato, K. L. Kuhen, C. Fischli, M. Rottmann, D. M. Plouffe, B. Bursulaya, S. Meister, L. Rameh, J. Trappe, D. Haasen, M. Timmerman, R. W. Sauerwein, R. Suwanarusk, B. Russell, L. Renia, F. Nosten, D. C. Tully, C. H. Kocken, R. J. Glynne, C. Bodenreider, D. A. Fidock, T. T. Diagana, E. A. Winzeler, *Nature* **2013**, *504*, 248 – 253.
[34] C. Doerig, O. Billker, T. Haystead, P. Sharma, A. B. Tobin, N. C. Waters, *Trends Parasitol.* **2008**, *24*, 570 – 577.
[35] MOE, The Chemical Computing Group Inc, Montreal, Canada, v2011, **2013**.

